**IJCRR**
Vol 04 issue 20
Section: General Science
Category: Research
Received on: 13/08/12
Revised on:04/09/12
Accepted on:21/09/12

# HYPERCHAOTIC BEHAVIOR OF A FIFTH-ORDER AUTONOMOUS ELECTRIC CIRCUIT

S. Manimaran[1], V. Balachandran[2], G. Kandiban[3]

[1]Department of Physics, Roever Engineering College, Perambalur , India
[2]Department of Physics, A. A Government Arts College, Musiri, Tiruchirappalli, India
[3]Department of Physics, Vivekanandha College of Arts and Sciences for Women, Tiruchengode, India

E-mail of Corresponding Author: brsbala@rediffmail.com

## ABSTRACT

In this paper, in order to show some interesting phenomena of fifth-order hyperchaotic autonomous electric circuit with a smooth cubic nonlinearity, different kinds of attractors, time waveforms and corresponding power spectra of systems are presented, respectively. The perturbation transforms an unpredictable hyperchaotic behavior into a predictable hyperchaotic or periodic motion via stabilization of unstable, aperiodic, or periodic orbits of the strange hyperchaotic attractor. One advantage of the method is its robustness against noise. A theoretical analysis of the circuit equations is presented, along with experimental simulation and numerical results.

**Keywords:** Fifth-order autonomous electric circuit; smooth cubic nonlinearity; chaos; hyperchaos.

## INTRODUCTION

Chaos and its related bifurcation phenomena have been an area of intense research in the last three decades. From the 1980s to the 1990s, simple and natural chaos generating circuits were proposed and laboratory experiments were carried out [1-5]. Matsumoto etal. insisted that their proposed circuits are natural (not artificial) circuits with only two terminal nonlinear elements. One of the major problems in this field is in the difficulty to prove the generation of chaos in a rigorous sense. A lot of researchers attempted to solve this problem by adopting simpler dynamics. As far as we know, one approach is based on the use of a singular perturbation (slow–fast) method, and the other is based on the use of a piecewise-linear technique [6-9]. Over the last two decades, hyperchaos has been intensively studied in many engineering-oriented applied fields, such as nonlinear circuits, secure communications, lasers, neural networks, control, synchronization, and so on. In chaotic secure communication, a chaotic signal is used to mask the message to be transmitted. As we know, the normal chaotic systems have one positive Lyapunov exponent. Perez and Cerderia proved that the messages masked by such a normal chaotic system are not always safe. However, Pecora found that this problem can be overcome by using the higher-dimensional hyperchaotic systems, which have an increasing randomness and higher unpredictability. In general, a hyperchaotic system is defined as a chaotic system with at least two positive exponents, implying that its dynamics are expended in several different directions simultaneously [7]. It means that hyperchaotic systems have more complex dynamical behaviors that can be used to improve the security of chaotic communication systems. Therefore, the theoretical design and circuitry realization of various hyperchaotic signals have recently become the focal research topics. Historically, hyperchaos was firstly reported by Rossler. That is, the noted four-dimensional (4D) hyperchaotic autonomous system. However, the hyperchaos was firstly discovered in electronic circuits by Matsumoto and his colleagues [5]. Over the last two decades, there are various hyperchaotic systems discovered in high-dimensional systems. Typical examples are hyperchaotic Rossler system, hyperchaotic Lorenz–Haken system, hyperchaotic Chua's circuit and hyperchaotic modified Chua's circuit [10-16].

Very recently, hyperchaos was found numerically and experimentally by adding a simple state feedback controller or a sinusoidal parameter perturbation controller in the generalized Lorenz system, Chen system, Lu system and a unified chaotic system. In this paper, a novel five-dimensional hyperchaotic system is constructed based on a modified autonomous Van der Pol Duffing oscillator [17]. The strong hyperchaotic nature is then verified by power spectrum, investigating its time waveforms and numerical confirmation. Furthermore, all above dynamical behaviors are verified by physically electronic circuit. Experimental observations are also given in this paper.

**Circuit Description and Simulation Results**

In order to understand chaotic circuit theory, it is important to consider the following problems: theoretical evidence for chaos, classification of chaos (e.g., classification by fractal dimension) and route to chaos [9]. These problems have been considered reasonably well for five dimensional circuits, but it is hard to analyze these problems in higher dimensional circuits. This paper considers these problems in a simple five-dimensional circuit of Fig. 1. Applying Kirchoff's laws, the set of five first-orders coupled autonomous differential equations as given below:

(1)

$$C_1 \frac{dV_1}{dt} = G_1 V_1 - i_N$$

$$C_2 \frac{dV_2}{dt} = i_N - i_{L_1}$$

$$C_3 \frac{dV_3}{dt} = i_{L_1} - i_{L_2}$$

$$L_1 \frac{di_{L_1}}{dt} = V_2 - V_3$$

$$L_2 \frac{di_{L_2}}{dt} = V_3$$

While $V_1$, $V_2$ and $V_3$ are the voltages across the Capacitors $C_1$, $C_2$ and $C_3$, $i_{L1}$ and $i_{L2}$ denotes the currents through the inductors $L_1$ and $L_2$ respectively and the characteristics of linear negative conductance is mathematically represented by $i_{G_1} = -G_1 V_1$. Here the term $i_N = f(V_1 - V_2)$ representing the characteristic of the smooth cubic nonlinearity can be expressed mathematically:

(2) $i_N = f(V_1 - V_2) = a(V_1 - V_2) + b(V_1 - V_2)^3$

For our present experimental study we have chosen the following typical values of the circuit in Fig. 1. Were $L_1$ = 33 *mH*, $L_2$ = 33 *mH*, $C_1$ = 85 *nF*, $C_2$ = 10 *nF*, $C_3$ = 100 *nF* and the characteristics of linear negative conductance $G_1$ = -0.5 *mS*. Here the variable capacitor '$C_1$' is assumed to be the control parameter. By decreasing the value of '$C_1$' from 85 *nF* to 45 *nF*, the circuit behavior of Fig. 1 is found to transit from a period-doubling route to chaos and then to hyperchaotic attractor through period-doubling bifurcation behavior followed by period-doubling windows and boundary crisis [15-16]. The hyperchaotic attractors of fifth-order autonomous circuit with the smooth cubic nonlinearity projected onto different planes are shown in Fig. 2. Experimental time series were registered using a simulation storage oscilloscope for discrete values of $C_1$ and $C_2$ are shown if Fig. 3.

The distribution of power in a signal *x(t)* is the most commonly quantified by means of the power density spectrum or simply power spectrum. It is the magnitude-square of the Fourier transforms of the signal *x(t)*. It can detect the presence of hyperchaos when the spectrum is broad-banded. The power spectrum corresponding to the voltages $V_1(t)$ and $V_2(t)$ waveforms across the capacitors $C_1$ and $C_2$ for the hyperchaotic regimes are shown in Fig. 4 which resembles broad-band spectrum noise.

**NUMERICAL CONFIRMATION**

The hyperchaotic attractor of fifth-order autonomous circuit as shown in Fig. 1 is studied by numerical integration of the normalized differential equations [14]. For a convenient numerical analysis of the experimental system given by Eqns. (1), we rescale the parameters as:

$$V_1 = Vx_1, V_2 = Vx_2, V_3 = Vx_3, i_{L_1} = \sqrt{\frac{C_1}{L_1}}Vx_4, i_{L_2} = \sqrt{\frac{C_1}{L_1}}Vx_5, \alpha_1 = a\sqrt{\frac{L_1}{C_1}}, \alpha_2 = b\sqrt{\frac{L_1}{C_1}}, \upsilon_1 = \frac{C_1}{C_2}, \upsilon_2 = \frac{C_1}{C_3}$$

$\gamma = G_1\sqrt{\frac{L_1}{C_1}}, \beta = \frac{L_1}{L_2}$, $t = \tau\sqrt{L_1 C_1}$ and then redefine τ as t. Eqns. (1) and (2) reduce to the following set of normalized equations of the fourth-order hyperchaotic autonomous electric circuit as given below:

(3)

$$\dot{x}_1 = \gamma x_1 - \alpha_1(x_1 - x_2) - \alpha_2(x_1 - x_2)^3$$

$$\dot{x}_2 = \upsilon_1(\alpha_1(x_1 - x_2) + \alpha_2(x_1 - x_2)^3 - x_4)$$

$$\dot{x}_3 = \upsilon_2(x_4 - x_5)$$

$$\dot{x}_4 = x_2 - x_3$$

$$\dot{x}_5 = \beta x_3$$

The dynamics of Eqns. (3) now depends upon the parameters $\alpha_1$, $\alpha_2$, $\upsilon_1$, $\upsilon_2$ $\gamma$, and $\beta$. The experimental results have been verified by numerical simulation of the normalized Eqns. (3) using the standard fourth-order Runge-Kutta method for a specific choice of system parameters employed in the experimental simulation results. That is, in the actual experimental set up the capacitor '$C_1$' is decreased from $C_1$ = 85 *nF* downward to 45 *nF*. Therefore in the numerical simulation, we study the corresponding Eqns. (3) for in the range $C_1$ = 85 *nF* to 45 *nF*. From our numerical investigations, we find that for the value of '$C_1$' below 85 *nF* periodic limit cycle motions is obtained. When the value of '$C_1$' is decreased to lower than 45 *nF* particularly in the range $C_1$ = (85 *nF* to 45 *nF*) the system displays a period-doubling route to chaos and then to hyperchaos through boundary condition [8]. These numerical results of the hyperchaotic attractor of fifth-order autonomous circuit with the smooth cubic nonlinearity projected onto different planes are shown in Fig. 5. Figure 6. Shows the numerical chaotic time series was registered using a discrete value of '$C_2$' serving as the control parameter. It is gratifying to note that the numerical results agree qualitatively very well with that of the experimental simulation results.

**CONCLUSIONS**

We have designed and investigated a hyperchaotic behavior of a fifth-order autonomous electric circuit. The circuit provides a higher bandwidth of strong chaotic signal with buffered output. Functionally was demonstrated using a commercial voltage feedback op-amp. Its simplicity arises from the fact that (i) The negative conductance is a simple op-amp impedance converter. (ii) The simple nonlinear element is synthesized from general purpose diode (1N4148 diode). (iii) The circuit equations are the most simple because of there is no locally active resistor (*R*) in the circuit, where the capacitance ($C_1$) as the control parameter. The attractive features of this circuit are the presence of period-doubling route to chaos and then to hyperchaos followed by period-doubling windows and boundary crisis etc. It is of further interest to study these aspects also in this system as well as the intermittency route to chaos and synchronization of coupled chaotic circuits of the present system for improved high security communication systems.

**REFERENCES**

1. I.M. Kyprianidis, I.N. Stouboulos, P. Haralabidis and T. Bountis *Int. J. Bifurc. and Chaos*. 8 (2000) 1903.
2. L.O. Chua and G.N. Lin *IEEE Trans. Circ. Syst*. CAS-38 (1991) 510.
3. M.P Kennedy *IEEE Trans. Circ. Syst. I.* 40 (1993) 640.
4. K. Murali and M. Lakshmanan *Int. J. Bifurc. and Chaos*. 1 (1991) 369.
5. T. Motsumoto, L.O. Chua and K. Kobaiashi, *IEEE Trans. Circ. Syst*. CAS-33 (1986) 1143.
6. A. Tamasevicius, A. Namajunas and A. Cenys *Electron. Lett*. 32 (1996) 957.
7. K. Thamilmaran, M. Lakshmanan and A. Venkatesan *Int. J. Bifurc. and Chaos*.14 (2004) 221.
8. R. Barboza *Int. J. Bifurc. and Chaos.* 18 (2008) 1151.
9. L.O. Chua and G.N. Lin *IEEE Trans. Circ. Syst.* 37 (1990) 885.
10. V. Balachandran and G. Kandiban *Indian J. Pure and Appl. Phys.* 47 (2009) 823.
11. A. Tamasevicius, A. Cenys, G. Mykolaitis, A. Namajunas and E. Lindberg *Electron. Lett.* 33 (1997) 542.
12. A. Tamasevicius and A. Cenys *Chaos, Solit. and Fract*. 9 (1998) 115.
13. C.L. Koliopanos, I.M. Kyprianidis, I.N. Stouboulos, A.N. Anagnostopoulos and L. Magafas *Chaos, Solit. and Fract.* 16 (2003) 173.
14. X. Liu, J. Wang and L. Huang *Int. J. Bifurc. and Chaos.* 17 (2007) 2705.
15. R. Barboza and L.O. Chua *Int. J. Bifurc. and Chaos.* 18 (2008) 943.
16. T. Kapitaniak and L.O. Chua *Int. J. Bifurc. and Chaos.* 4 (1994) 477.
17. G.P. King and S.T. Gaito *Phys. Rev. A.* 46 (1992) 3093.

**Figure 1. Circuit realization of the fifth-order hyperchaotic autonomous electric circuit**

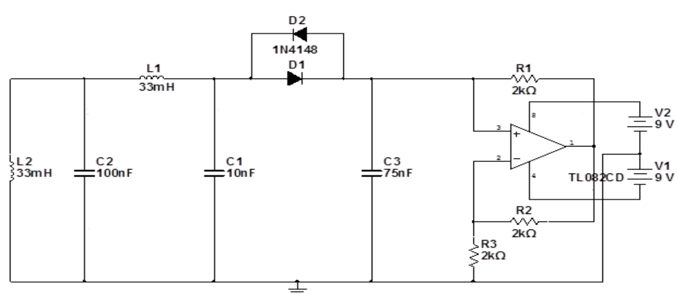

**Figure 2. Simulation results of the projections of hyperchaotic attractor onto different planes**

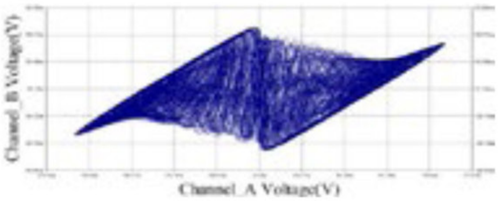


**(a**

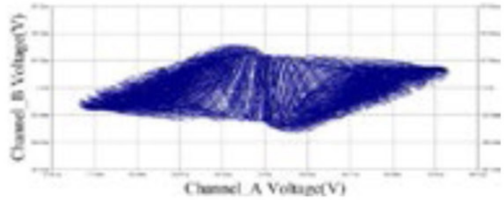


**(b**

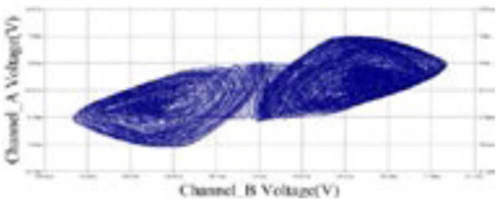


**(c**

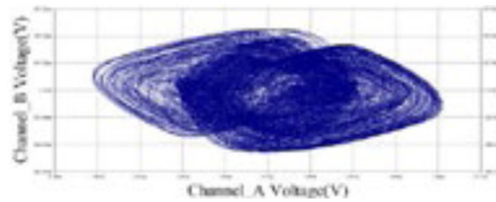


**(d**

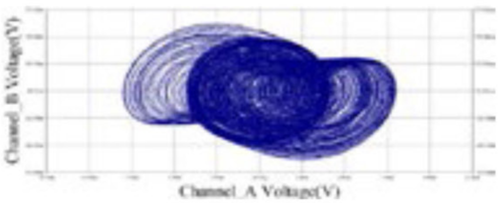


**(e**

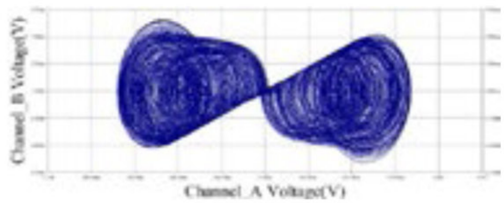


**(f**

**Figure 3. Simulation results of the hyperchaotic time series**

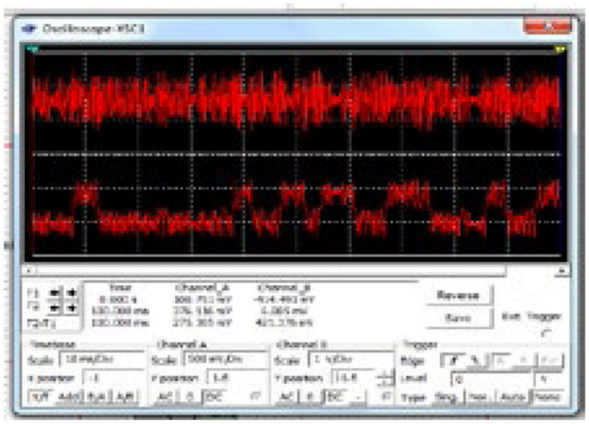

**Figure 4. Simulation results of the projections of hyperchaotic power spectrum**

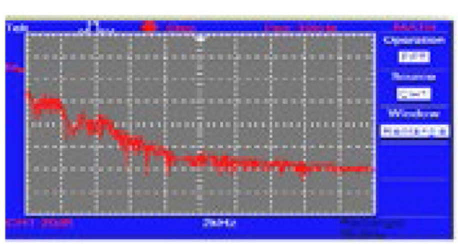

(a)

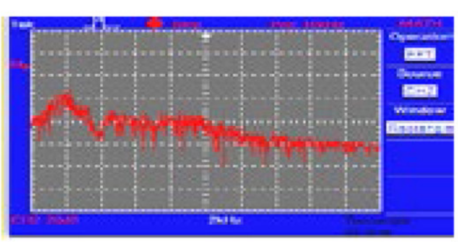

(b)

**Figure 5. Numerical results of the projections of hyperchaotic attractor onto different planes**

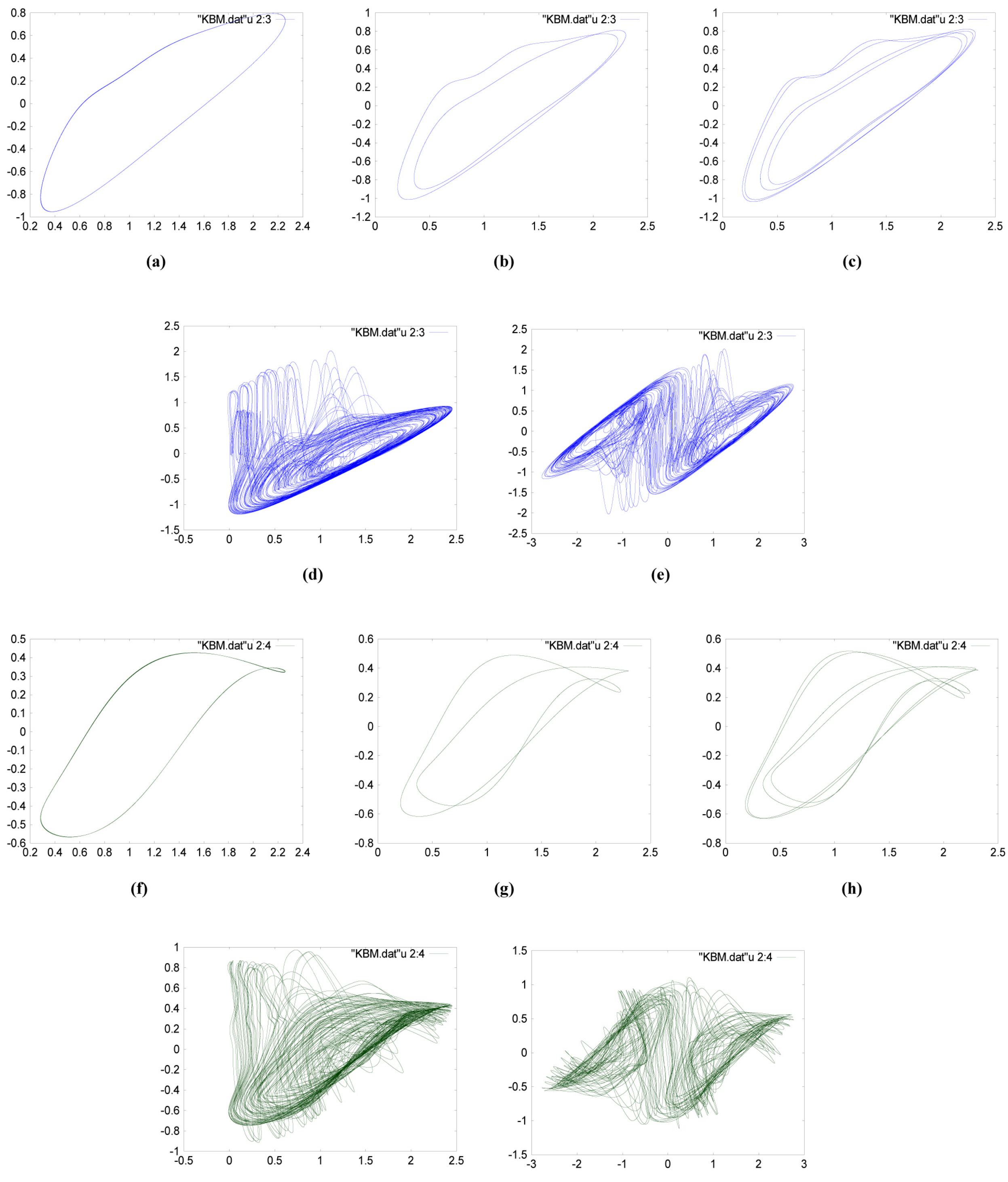


(a) (b) (c)

(d) (e)

(f) (g) (h)

(i) (j)

**Figure 6. Numerical results of the hyperchaotic time series**

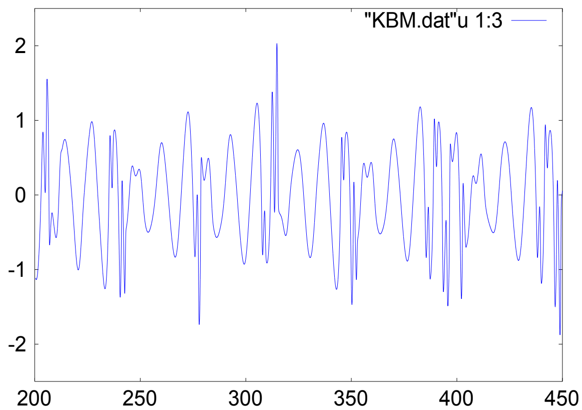


**(a)**

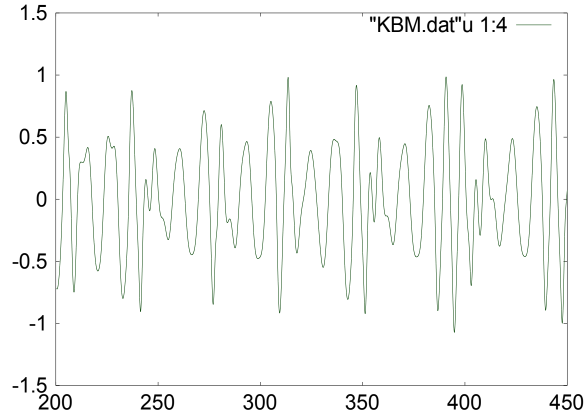


**(b)**